Energy 105 (2016) 45–56

Contents lists available at ScienceDirect

Energy

journal homepage: www.elsevier.com/locate/energy

# Cold energy utilization of liquefied natural gas for capturing carbon dioxide in the flue gas from the magnesite processing industry

Liang Zhao [a], Hui Dong [a,*], Jiajun Tang [b], Jiuju Cai [a]

[a] SEP Key Laboratory of Eco-Industry of Northeastern University, Shenyang 110819, China
[b] Institute of Refrigeration and Cryogenics, Shanghai Jiao Tong University, Shanghai 200240, China

A R T I C L E I N F O

*Article history:*
Received 5 January 2015
Received in revised form
27 August 2015
Accepted 29 August 2015
Available online 26 September 2015

*Keywords:*
LNG (liquefied natural gas)
$CO_2$ capture
Cold energy
ORC power generation
Exergy analysis
$CO_2$ utilization

A B S T R A C T

In the present paper, a novel system based on LNG (liquefied natural gas) cold energy utilization was proposed to capture $CO_2$ in the exhaust gas discharged from the magnesite processing industry located in Liaoning Province (China). The system also combined with a twin-stage ORC (organic Rankine cycle) power generation sub-system using LNG as heat sink and exhaust gas as heat source. Based on the exergy analysis method, the LNG regasification pressure and the $CO_2$ capture pressure were investigated as the key operation parameters to find the suitable working conditions of the system. The results show that, in Liaoning Province, the amount of LNG cold energy received at Xianrendao Port can theoretically afford to capture $CO_2$ in the exhaust gas from the magnesite processing industry at Dashiqiao Area. In addition, when the LNG regasification pressure and the $CO_2$ capture pressure is respectively set as 1.0 MPa and 0.15 MPa, the system can reach exergy efficiency of 0.57 and provide 119.42 kW electric power and 0.75 t liquid $CO_2$ per ton LNG. For downstream utilization of $CO_2$, a $CO_2$ utilization sub-system was proposed. It integrates Rankine cycle, water electrolysis and carbon dioxide hydrogenation for methanol production by solar energy and liquefied $CO_2$ cold energy utilization.



## 1. Introduction

As the world continuously develops, the conflict between environment problems and energy sector has become more and more obvious. NG (natural gas) is a kind of environment friendly resource with high conversion within the combustion process [1]. Thus, using NG instead of other traditional fossil fuels for energy supply is considered as a suitable way to ease this contradiction.

LNG (liquefied natural gas) is the main transportation form of long-range transport by water transportation and short-range ground transportation. In addition, during the liquefied process, LNG contains enormous cold energy (or cryogenic energy) which consists of low temperature (about 110 K) sensible heat and latent heat of vaporization. The cold energy can be released during the regasification process of LNG. That means, LNG can be used as a chemical energy resource and also as a cold energy resource. However, the conventional regasification systems squander the cold energy but require significant energy supply [2]. Therefore, many researchers focus on developing some methods to recover the cold energy during the LNG regasification process.

Among the methods for recovering cold energy, electricity power generation is one of the most efficient way. About 15 cryogenic power plants using cold energy of LNG have been built in Japan since 1979 to 2000 [3]. In the past three decades, the performances of those cryogenic power plants have been constantly improved. Dispenza [4,5] proposed an innovative process which used a cryogenic stream of LNG during regasification as cold source in an improved CHP (combined heat and power) modular plant. Szargut [6] investigated the efficiency differences between three variant types of cryogenic power plant by some key parameters including ambient temperature, heat transfer temperature difference etc. Consequently, the production of electricity power recovering the available cold energy during LNG regasification process, should be a very suitable option for an improved power plant or in a cryogenic power plant. Therefore, lots of researches put emphasis to increase the efficiency of LNG cold energy utilization for power generation by combining traditional power cycles or with further optimization of some key parameters of these cycles. Choi [7] proposed a cascade Rankine cycle with propane as the working fluid for recovering LNG cold energy for power generation. The process simulation indicated that the parameters such as net power output, energetic efficiency,

* Corresponding author. Fax: +86 024 83672218.
*E-mail addresses:* zhliang8341@163.com, Dongh@smm.neu.edu.cn (H. Dong).

http://dx.doi.org/10.1016/j.energy.2015.08.110
0360-5442/

and exergy efficiency generally increased as the number of stages increases (≤3 stages). Gómez [8] presented a novel power plant consisting of a combination of a CBC (closed Brayton cycle) with a SRC (steam Rankine cycle) while exploiting the cold exergy available in the regasification process of LNG. An energy and exergy analysis was also carried out to evaluate the effect of some key parameters on the efficiency. Still Gómez [2], carried out a review of the current state of thermodynamic cycles for improving power generation efficiency by using cold energy during LNG regasification process, and also established a selection criteria of the working fluids. Dong [9] fundamentally investigated a method which utilized LNG cold energy for power generation with Stirling cycle based on previous studies, and made some improvements of the method.

The power generation performance is, however, significantly affected by the thermodynamic properties of the working fluids. As a consequence, some researches focus on investigating the working fluid properties to find the more suitable one [10] (or a group [11–13]) for recovering cold energy of LNG. Indeed, carbon dioxide ($CO_2$) is also a feasible choice for power generation cycle with utilization of LNG cold energy [14,15]. It indicates that LNG with low temperature can be regarded as a heat sink to condense the $CO_2$ under the specific conditions. It could be a good solution to some environmental problems such as global warming and rising sea levels, that utilizing LNG cold energy to capture $CO_2$. Therefore, some researchers have studied about capturing $CO_2$ though cold energy recovery in LNG fueled power plant. Liu [16] presented a thermo-economic analysis aimed at the optimization of a novel zero-$CO_2$ and other emissions and high-efficiency power and refrigeration cogeneration system. Zhang [17] presented a novel scheme of LNG fueled power plant, which could liquefy $CO_2$ after combustion process and capture it from the cycle without consuming additional power. Alabdulkarem [18] integrated a LNG plant with a CCS ($CO_2$ capture and sequestration) plant for recovering waste heat to reduce energy consumption during $CO_2$ liquefaction process. These researches about $CO_2$ capture of power generation system were focused on 'self-capture' system which belongs to post capture system. However, some industries also can produce large amounts of carbon dioxide without combustion, for instance, the magnesite processing industry.

Magnesite ($MgCO_3$) processing industry in China, particularly in Liaoning Province, is another bulky $CO_2$ emission source which could avoid separating process to reducing energy consumption. According to the U.S. Geological Survey [19], there is a large amount of magnesite mine reserves in China (20.9% of total world). Most magnesite mine resources in China (85.5% of total China) are discovered at west and south of Liaoning Province, especially at Yingkou City (over 30%) [20]. For long time, magnesite processing industry has been widely pullulated in Liaoning Province. Over hundreds of enterprises are specialized in magnesite processing, and the total production of these companies can reach to 7.87 million tons per year [21]. Approximately, almost 4 million tons of $CO_2$, which accounts for 1% of total carbon emission in Liaoning Province will be discharged to the environment [22]. The mechanism of $CO_2$ generation process in a magnesite processing plant is inherently different in a power generation plant. The magnesite is heated by electric arc in a pillar furnace and decomposed to MgO and $CO_2$. There are two types of electric arc furnace used by magnesite processing plant: open-type and closed-type. The closed-type furnace puts a moving petticoat pipe structure on the mouth of furnace when the magnesite is heating in the furnace. Thus, the flue gas can be effectually centralized for subsequent treatment, such as dust removal [23]. As a consequence, the concentration of $CO_2$ in the centralized flue gas from a closed-type furnace is higher than it in the uptight flue gas from an open-type furnace. Some test results shows that the $CO_2$ volume fraction in the flue gas of the open-type furnace is 0.31 on average [21]. Recently, three closed-type furnaces of different magnesite processing plants at Yingkou City were chosen for testing the $CO_2$ concentration of flue gas. The results show that the $CO_2$ volume fraction in the flue gas of the closed-type furnace reaches 0.40–0.49. Because of the negative pressure environment needed by the dust control system, a large quantity of air that can be inhaled though unsealed places, such as the joints of pipe. For this reason, it is difficult to get $CO_2$ volume fraction over 0.50 in the flue gas of the closed-type furnace.

In China, $CO_2$ capture is concentrated in power generation system because of 73% of the total carbon emissions come from this sector [24]. Post-combustion $CO_2$ capture and oxy-fuel combustion are two basic technologies for capturing $CO_2$ from power systems [25]. Until now, the major obstacle deterring the development of $CO_2$ capture technology is high-energy penalty for separating $CO_2$ from flue gas [26]. Therefore, concentrating $CO_2$ in flue gas is the first and main energy consumption process of $CO_2$ capture. LNG cold energy can be utilized as energy supplement for $CO_2$ capture process. Nevertheless, the research is still blank that utilize LNG cold energy for capture $CO_2$ from magnesite processing industry in Liaoning Province.

In this paper, a novel system of LNG cold energy utilization for generating power and capturing $CO_2$ is proposed. The system combines a power generation sub-system which consists of two organic Rankine cycles both considered LNG as heat sink and the flue gas as heat source. The mathematical model of the system is established to calculate the thermodynamic parameters of the system. And then, the model is applied to evaluate a real case in Liaoning Province, China. In this case, $CO_2$ in flue gas from magnesite processing industry located at Dashiqiao Area will be captured by LNG cold energy located at Xianrendao Port. In addition, the sensitive analysis of some key operation parameters is conducted to examine the system performance for finding the suitable working conditions. Furthermore, the feasibility analysis is made for a $CO_2$ utilization sub-system for methanol production.

## 2. System description

The specific system design of LNG cold energy utilization for power generation and $CO_2$ capture is shown in Fig. 1. $CO_2$ is liquefied within this system using LNG cold energy recovery. The system employs the flue gas from the magnesite processing industry as heat source to supply heat energy to a parallel twin-stage Rankine cycle, which considering LNG as heat sink to generating power. This overall system consists of a $CO_2$ capture sub-system, a twin-stage organic Rankine cycle power generation sub-system and a LNG regasification sub-system.

The $CO_2$ capture sub-system consists of a $CO_2$ compressor, two heat exchangers and a liquid–vapor separator. The flue gas, firstly, is compressed by the compressor for overcoming the pressure drops within heat exchangers. Then, the flue gas is cooled down in two heat exchangers respectively. Finally, $CO_2$ is liquefied though releasing heat to Rankine cycle and separated from air in the liquid–vapor separator. The waste heat of the flue gas is the only heat source for heat energy supply to the power generation sub-system. The process is shown as C1 to C6. C5 and C6 denotes air and liquefied $CO_2$, respectively.

For using LNG cold energy efficiently and simplifying the overall system, a parallel twin-stage organic Rankine cycle is selected for power generation sub-system. Though organic Rankine cycle is a widely option for generating power associated with LNG regasification process, a working fluid with appropriate physical properties should be used [8]. According to the working conditions of the

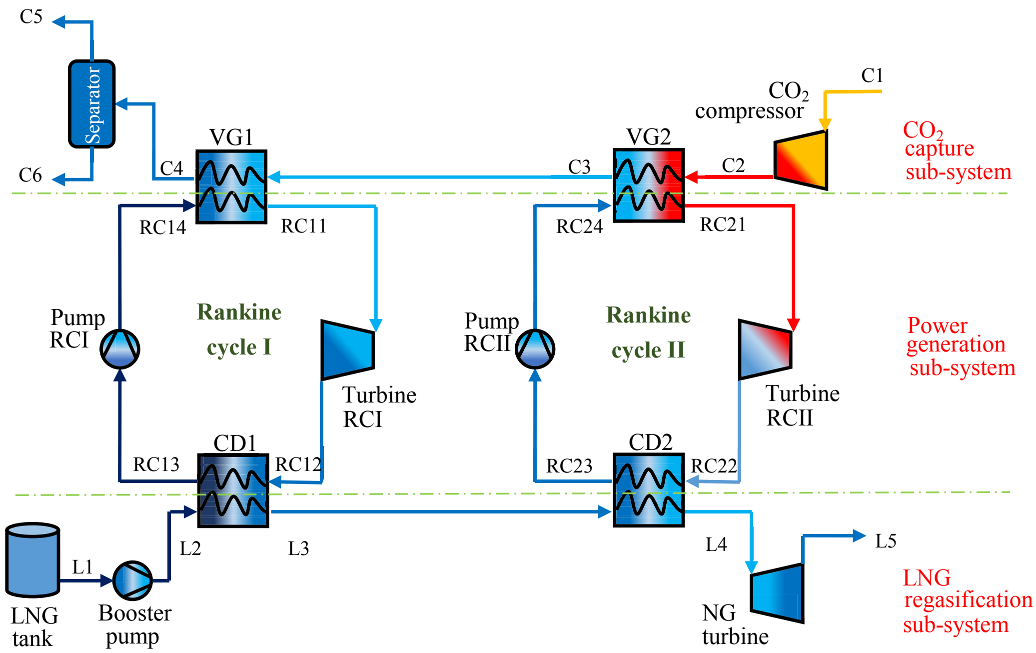


**Fig. 1.** The system scheme design of combined $CO_2$ capture and cold energy generation.

system in this paper and the working fluids election criteria proposed by Gómez [2], R-14 (Tetrafluoromethane) and R-290 (Propane) is chosen for Rankine cycle I and II as working fluid, respectively. Each Rankine cycle consists of a pump, a vapor generator, a turbine and a condenser. The working fluid is compressed by the pump, and then enters the vapor generator. In the vapor generator the working fluid is vaporized by absorbing heat from the flue gas. Then, the high-temperature working fluid flows into a turbine, where it expands to produce mechanical power to drive an electric generator. At last, the exhaust working fluid is condensed in a condenser by LNG after leaving the turbine. The two Rankine cycles are shown as RC11 to RC14 and RC21 to RC24, respectively.

The LNG regasification sub-system consists of LNG tank, LNG booster pump, heat exchangers and NG turbine. LNG with low temperature of −162 °C is drawn out from the LNG tank and pumped to regasification pressure. Then LNG enters the condensers of two Rankine cycles and absorbs heat from R-14 and R-290 respectively. Thus, LNG is vaporized to natural gas through absorbing heat from the working fluids and releases the cold energy to condense the working fluids. Finally, the natural gas enters NG turbine to produce electric power and decreases the pressure for the city gas pipeline. The process is shown as L1 to L5.

## 3. Mathematical modeling

Among many state equations, the P–R (Peng-Robinson) equation is more suitable for calculating the physical properties both of mixtures [27] and pure substances [28]. Therefore, P–R equation is chosen for calculating the thermodynamic and thermo-physical properties for LNG as well as for $CO_2$, R-14 and R-290.

The following assumptions are made to simplify the modeling of the system.

(1) LNG composition consists of methane, ethane, propane and nitrogen. The molar concentration is 90.38%, 5.37%, 4.04% and 0.21% respectively [9].
(2) The pressure drop of LNG regasification sub-system is assumed to be equal to 3% [15]. Therefore, the pressure drops through the vapor generators and condensers of power generation sub-system is also considered as 3%.
(3) Heat transfer between the environment and the system is neglected.
(4) The isentropic efficiency of turbine, pump and compressor is equal to 0.9.
(5) The volume fraction of $CO_2$ in the flue gas is considered as 0.45.

### 3.1. $CO_2$ capture sub-system

In the $CO_2$ capture system, the flue gas is cooled down by R-14 and R-290 respectively.

The heat released to R-14 in the Vapor-generator 1 is calculated by

$$Q_{flue\ gas,\ VG1} = m_{flue\ gas}(h_{C4} - h_{C3}) \tag{1}$$

The heat released to R-290 in the Vapor-generator 2 is

$$Q_{flue\ gas,\ VG2} = m_{flue\ gas}(h_{C3} - h_{C2}) \tag{2}$$

For overcoming the pressure drops in the heat exchangers, the flue gas is compressed by a compressor.

The compressor power consumption is

$$W_{compressor,\ flue\ gas} = m_{flue\ gas}(h_{C2} - h_{C1}) \tag{3}$$

### 3.2. ORC power generation sub-system

#### 3.2.1. Rankine cycle I

Rankine cycle is a classic thermodynamic cycle for power generation. It consists of two heat exchangers, pump and turbine. The mechanical power can be obtained by Rankine cycle when heat is allowed to flow from a heat source to a heat sink.

The heat absorbed by R-14 from the flue gas in the Vapor-generator 1 is calculated as follow

$$Q_{R-14,\ VG1} = m_{R-14}(h_{RC11} - h_{RC14}) = Q_{flue\ gas,\ VG1} \tag{4}$$

The heat discharged from R-14 to LNG in the Condenser 1 is

$$Q_{R-14,\ CD1} = m_{R-14}(h_{RC13} - h_{RC12}) \tag{5}$$

The pump power consumption in the Rankine cycle I is

$$W_{pump,\ RC1} = m_{R-14}(h_{RC14} - h_{RC13}) \tag{6}$$

The mechanical power generated by the R-14 turbine is

$$W_{turbine,\ RC1} = m_{R-14}(h_{RC12} - h_{RC11}) \tag{7}$$

Thus the net power output of the Rankine cycle I can be calculated by

$$W_{net,\ RCI} = W_{turbine,\ RCI} - W_{pump,\ RCI} \tag{8}$$

#### 3.2.2. Rankine cycle II

The mathematic model of Rankine cycle II is similar as Rankine cycle I, and given as bellow.

The heat absorbed by R-290 from the flue gas in the Vapor-generator 2 is calculated as follow

$$Q_{R-290,\ VG2} = m_{R-290}(h_{RC21} - h_{RC24}) = Q_{flue\ gas,\ VG2} \tag{9}$$

The heat discharged from R-290 to LNG in the Condenser 1 is

$$Q_{R-290,\ CD2} = m_{R-290}(h_{RC23} - h_{RC22}) \tag{10}$$

The pump power consumption in the Rankine cycle II is

$$W_{pump,\ RC2} = m_{R-290}(h_{RC24} - h_{RC23}) \tag{11}$$

The mechanical power generated by the R-290 turbine is

$$W_{turbine,\ RC2} = m_{R-290}(h_{RC22} - h_{RC21}) \tag{12}$$

Thus the net power output of the Rankine cycle II can be calculated by

$$W_{net,\ RCII} = W_{turbine,\ RCII} - W_{pump,\ RCII} \tag{13}$$

### 3.3. LNG regasification sub-system

LNG is boosted up by the pump and vaporized in two heat exchangers though absorbing heat from Rankine cycle I and II.

The heat absorbed by LNG from R-14 in the Condenser 1 is calculated as follow

$$Q_{LNG,\ CD1} = m_{LNG}(h_{L3} - h_{L2}) = Q_{R-14,\ CD1} \tag{14}$$

The heat absorbed by LNG from R-290 in the Condenser 2 is

$$Q_{LNG,\ CD2} = m_{LNG}(h_{L4} - h_{L3}) = Q_{R-290,\ CD2} \tag{15}$$

The booster pump power consumption is

$$W_{pump,\ LNG} = m_{LNG}(h_{L2} - h_{L1}) \tag{16}$$

At last, LNG is fully vaporized and expanded to low pressure by a turbine for city gas pipeline.

The mechanical power generated by the NG turbine is

$$W_{turbine,\ NG} = m_{LNG}(h_{L5} - h_{L4}) \tag{17}$$

Thus the net power output of the LNG regasification sub-system can be calculated by

$$W_{net,\ LNG} = W_{turbine,\ NG} - W_{pump,\ LNG} \tag{18}$$

### 3.4. The exergy analysis of the overall system

Some thermodynamic parameters of the overall system, such as net power output, exergy efficiency and specific quantity of $CO_2$ recovery are calculated for analyzing the performance of the system.

The net power output of the overall system is calculated by

$$W_{net,\ overall} = W_{net,\ RCI} + W_{net,\ RCII} + W_{net,\ LNG} - W_{compressor,\ CO_2} \tag{19}$$

Due to the deterioration of energy quality cannot be reflected by the energy method based on the first thermodynamic law, there is considerable interest in using an exergy analysis in thermodynamic analyses of thermal systems [29]. Exergy is defined as the maximum theoretical work obtainable from a system in disequilibrium with the reference environment. Exergy is consists of physical exergy and chemical exergy. There is no chemical reaction in the system proposed in this paper, thus, exergy investigated in the system is especially the physical exergy.

The exergy at a state point of a substance can be defined as

$$E = m[(h - h_0) - T(s - s_0)] \tag{20}$$

where, $h_0$ and $s_0$ is enthalpy and entropy of the reference state, respectively.

Once the exergy at state points are decided, the exergy losses of both heat exchangers and power machines can be calculated.

The exergy loss in the Vapor-generator 1 is

$$I_{VG1} = E_{C3} + E_{RC14} - E_{C4} - E_{RC11} \tag{21}$$

Similarly, the exergy loss in the Vapor-generator 2 is

$$I_{VG2} = E_{C2} + E_{RC24} - E_{C3} - E_{RC21} \tag{22}$$

The exergy loss in the Condenser 1 is

$$I_{CD1} = E_{RC12} + E_{L2} - E_{RC13} - E_{L3} \tag{23}$$

Similarly, the exergy loss in the Condenser 1 is

$$I_{CD2} = E_{RC22} + E_{L3} - E_{RC23} - E_{L4} \tag{24}$$

The exergy loss in the LNG booster pump is

$$I_{pump,\ LNG} = E_{L1} + W_{pump,\ LNG} - E_{L2} \tag{25}$$

The exergy loss in the pump of Rankine cycle I is

$$I_{pump,\ RCI} = E_{R13} + W_{pump,\ RCI} - E_{R14} \tag{26}$$

The exergy loss in the pump of Rankine cycle II is

$$I_{pump,\ RCII} = E_{RC23} + W_{pump,\ RCII} - E_{RC24} \tag{27}$$

The exergy loss in the turbine of Rankine cycle I is

$$I_{turbine,\ RCI} = E_{RC11} - W_{turbine,\ RCI} - E_{RC12} \tag{28}$$

The exergy loss in the turbine of Rankine cycle II is

$$I_{turbine,\ RCII} = E_{RC21} - W_{turbine,\ RCII} - E_{RC22} \tag{29}$$

The exergy loss in the $CO_2$ compressor is

$$I_{compressor,\ CO_2} = E_{C1} + W_{compressor,\ CO_2} - E_{C2} \tag{30}$$

The exergy loss in the NG turbine is

$$I_{turbine,\ NG} = E_{L4} - W_{turbine,\ NG} - E_{L5} \tag{31}$$

When the exergy loss of each device is determined, the exergy efficiency also can be evaluated.

The exergy efficiency of a system is

$$\eta = E_{gain}/E_{pay} \tag{32}$$

The exergy efficiency of the overall system is

$$\eta_{overall} = \frac{W_{net,\ overall} + E_{CO_2}}{E_{flue\ gas} + E_{LNG}} \tag{33}$$

where,

$$E_{flue\ gas} = m_{flue\ gas}[(h_{C1} - h_{C0}) - T_0(s_{C1} - s_{C0})] \tag{34}$$

$$E_{LNG} = m_{LNG}[(h_{L1} - h_{L0}) - T_0(s_{L1} - s_{L0})] \tag{35}$$

$$E_{CO_2} = m_{C6}[(h_{C6} - h_{C0}) - T_0(s_{C6} - s_{C0})] \tag{36}$$

The specific quantity of $CO_2$ recovery is defined as the amount of $CO_2$ captured divide by the consumption of LNG in the overall system. It can be expressed as

$$\alpha = m_{C6}/m_{LNG} \tag{37}$$

## 4. Case description

Yingkou City in Liaoning Province (China) is selected as the case city to conduct the numerical simulation, because of the reserves in Yingkou City is a third of Liaoning Province. Xianrendao Port and Dashiqiao Area are two of administrative regions of Yingkou City. The Yingkou LNG receiving terminal is located at Xianrendao Port, 60 km south of downtown. Magnesite processing industry is converged at Dashiqiao Area, 20 km east of downtown.

There are two LNG receiving terminals in Liaoning Province by now. The Dalian terminal has operated for three years since 2011. The maximum unload capacity of its berth to accommodate supply ships can reach to 10.25 Mt/a LNG, which is the largest size in China [30]. The Yingkou terminal is still under construction and expected to go into operation in 2017. It features three tanks, each capable of holding 0.16 $Mm^3$ of LNG and a berth to accommodate a supply ship. Its unload capacity of LNG can be 3 Mt/a [31]. There are two sources of LNG at Xianrendao Port: ① Imported by LNG ships from other producer countries and received by onshore terminal; ② Transported through submarine pipeline from offshore drilling platform (#Jinzhou 25-1 south) to onshore liquefied plant. On account of controlling transportation distance and cost, LNG from Yingkou receiving terminal at Xianrendao Port is chosen as cold energy source for $CO_2$ capture and power generation at Dashiqiao Area.

There are three kinds of product of magnesite processing, caustic magnesite, dead-burned magnesite and fused magnesite. According to the total amount of magnesite processing production capacity in Dashiqiao Area (2013) [23], 2.8 million tons of caustic magnesite (37.7%), dead-burned magnesite (32.9%) and fused magnesite (29.4%) have been produced. No matter which product, $CO_2$ is always decomposed from the heating process of magnesite ore in the electric arc furnace. Thus, according to the chemical reaction formula, shown as Eq. (38), almost 1.4 million tons of $CO_2$ have been discharged from magnesite processing industry in Dashiqiao Area during a year.

$$MgCO_3 \rightarrow MgO + CO_2 \tag{38}$$

In this paper, the LNG imported at Xianrendao Port is transported to Dashiqiao Area for $CO_2$ capture and power generation. A scheme is proposed as shown in Fig. 2. LNG is received by onshore terminal or produced by liquefaction plant. Then, LNG is uploaded with tank trucks and moved north to Dashiqiao Area through highway. In LNG satellite station at Dashiqiao Area, the generators are driven by Rankine cycle using LNG as heat sink and exhaust gas from the electric furnace as heat source. $CO_2$ in the exhaust gas from magnesite processing industry at Dashiqiao Area is captured and liquefied by LNG cold energy. The captured $CO_2$ is used in the $CO_2$ utilization sub-system for methanol production.

## 5. Results and discussion

The thermodynamic parameters of working fluids, including entropy, enthalpy and vapor fraction etc., are calculated by the model proposed in Ref. [9]. In this section, based on the exergy analysis method, the thermodynamic performance of the system is studied. In addition, LNG regasification pressure and $CO_2$ capture pressure are two key operation parameters of the system. Therefore, the effects of these two parameters on the performance of the system are investigated.

The *T-s* diagram of the overall system is shown in Fig. 3. The two ORCs are arranged above the LNG regasification period successively for recovering cold energy adequately. The flue gas from magnesite processing industry is set as the heat source of the ORCs. The $CO_2$ in the flue gas is cooled down by ORCs respectively. The initial data for the simulation of the system are listed in Table 1.

### 5.1. Exergy analysis

The reference state for exergy calculations is set as $T_0 = 298.15$ K and $p_0 = 0.101$ MPa. The calculation results of exergy input, output and loss of the system under the initial conditions, are shown in Table 2. It can be seen that the exergy input contains exergy of flue gas, exergy of LNG and electric power input though compressor and pumps. The exergy output includes exergy of $CO_2$, the mechanical work produced by the ORC power generation sub-system and also produced by NG turbine of the LNG regasification sub-system. The percentages of exergy loss of all the system components are shown in Fig. 4, including vapor-generators, condensers, pumps, turbines and compressor. Because of the temperature difference in heat transfer process, the mainly exergy losses within the heat exchangers is the mainly exergy losses of the system (more than 93%). The other exergy losses in the components exist in the pumps and turbines are caused for the irreversibility of process (less than 7%).

For analyzing the exergy losses in the heat exchangers, the temperature differences under the initial conditions in the vapor-generators and condensers are calculated and shown in Fig. 5. The LMTD (log mean temperature differences) of VG1, VG2, CD1 and CD2 are 5.67 K, 11.69 K, 7.26 K and 10.55 K, respectively. Although large temperature difference can enhance the irreversible effect in heat transfer process, it is not the only influential factor of exergy loss. This phenomenon can be seen in Fig. 4. However the LMTD is minimum among the heat exchangers, the largest exergy loss of VG1 (about 37%) results from the large amount of flue gas exergy input. The compression and expansion processes of compressors (or pumps) and turbines are almost isentropic, accordingly the exergy losses within these components are the non-principal

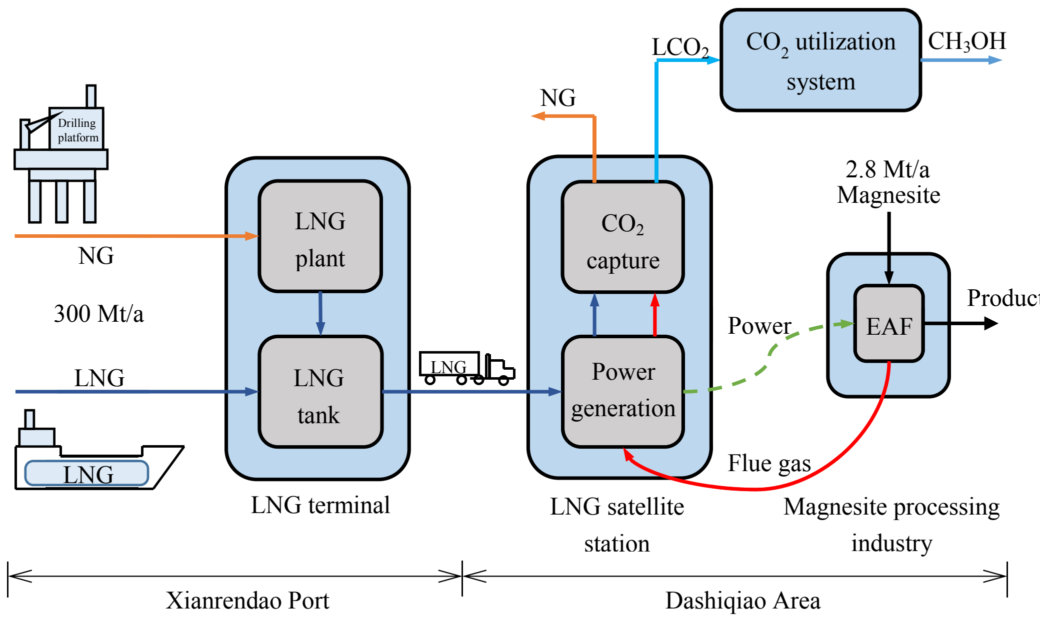


**Fig. 2.** The overall scheme of LNG cold energy from Xianrendao Port utilized by magnesite processing industry in Dashiqiao area.

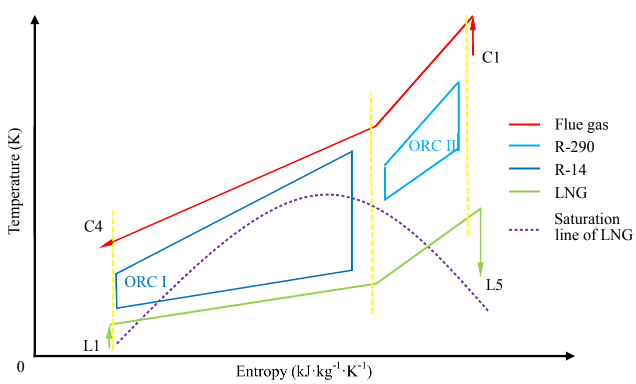


**Fig. 3.** *T-s* diagram of LNG regasification and power generation system.

aspects of exergy loss within the overall system. The similar results are also found by Xia [32].

The exergy efficiency of the overall system calculated by Eq. (33) is 0.52 at the initial conditions. The reason of low exergy efficiency is the exergy losses in the components of the system. On the other hand, low concentration of $CO_2$ in the flue gas also leads to low exergy efficiency of the system. Air is cooled down with $CO_2$ by the system cause of the flue gas is a mixture of $CO_2$ and air. However, abundant exergy floods out of the system attaching the cooled air with low temperature and high pressure. Using the terminational air after the liquid–vapor separator as the ingredient of an air separation system may be a feasible means to decrease the exergy loss caused by low concentration of $CO_2$. The further work will be followed up.

**Table 1**
The initial modeling conditions of the system.

| Overall system | |
|---|---|
| Ambient temperature (K) | 298.15 |
| Ambient pressure (MPa) | 0.101 |
| Heat exchanger pressure drop (MPa) | 0.003 |
| Pump adiabatic efficiency | 0.95 |
| Compressor adiabatic efficiency | 0.95 |
| Turbine adiabatic efficiency | 0.95 |
| **$CO_2$ capture subsystem** | |
| $CO_2$ volume fraction | 0.45 |
| Air volume fraction | 0.55 |
| $CO_2$ compressor inlet temperature (K) | 325.15 |
| $CO_2$ compressor inlet pressure (MPa) | 0.10 |
| $CO_2$ compressor outlet pressure (MPa) | 0.15 |
| C3 temperature (K) | 255.15 |
| C4 temperature (K) | 163.15 |
| **ORC power generation subsystem** | |
| RC1 pump inlet temperature (K) | 113.15 |
| RC1 pump inlet pressure (MPa) | 0.185 |
| RC1 pump outlet pressure (MPa) | 0.40 |
| RC1 turbine inlet pressure (MPa) | 0.397 |
| RC1 turbine outlet pressure (MPa) | 0.188 |
| RC2 pump inlet temperature (K) | 173.15 |
| RC2 pump inlet pressure (MPa) | 0.13 |
| RC2 pump outlet pressure (MPa) | 0.90 |
| RC2 turbine inlet pressure (MPa) | 0.897 |
| RC2 turbine outlet pressure (MPa) | 0.133 |
| **LNG regasification subsystem** | |
| Mass flow rate of LNG (kg $s^{-1}$) | 1.0 |
| LNG booster pump inlet temperature (K) | 111.15 |
| LNG booster pump inlet pressure (MPa) | 0.10 |
| LNG booster pump outlet pressure (MPa) | 0.60 |
| NG turbine inlet pressure (MPa) | 0.594 |
| NG turbine outlet pressure (MPa) | 0.15 |
| L3 temperature (K) | 168.15 |

### *5.2. Sensitivity analysis of key parameters on the system performance*

#### *5.2.1. The LNG regasification pressure*

The LNG regasification pressure is a very sensitive parameter in the release process of LNG cold energy. The effect of LNG regasification pressure on network output and exergy loss of the system is shown in Fig. 6. It can be seen that along with the increase of LNG regasification pressure, the network output of the overall system increases first and then decreases; the exergy loss of the overall system is straight going down.

The mainly reason of this phenomenon is that the LNG regasification pressure significantly affect the work output of NG turbine (seen in Fig. 7). The variation trend of NG turbine work output is similar with the network output of the overall system. In addition,

**Table 2**
The calculation results of exergy input, output and loss in the system.

| Term | Value (kW) |
|---|---|
| **Exergy input** | 1068.83 |
| LNG (L1) | 962.94 |
| $CO_2$ (C1) | 3.09 |
| $CO_2$ compressor | 100.80 |
| LNG booster pump | 1.14 |
| RC1 pump | 0.36 |
| RC2 pump | 0.50 |
| **Exergy output** | 557.04 |
| LNG (L5) | 114.84 |
| $CO_2$ (C6) | 235.78 |
| NG turbine | 126.94 |
| RC1 turbine | 38.76 |
| RC2 turbine | 40.72 |
| **Exergy loss** | 551.79 |
| Air (C5) | 247.22 |
| Devices of the system | 304.57 |
| **Exergy efficiency** | 0.52 |

when LNG regasification pressure is 0.15 MPa which equal to city gas supply pressure, the NG turbine is not working. Thus, the network output of the overall system is minimum at that regasification condition. The network output is negative means that the system requires work input for operating. Besides, the work output of turbines in the two ORCs is inconspicuously affected by the LNG regasification pressure.

The most work consumption unit is the $CO_2$ compressor whose work input gently decreases with LNG regasification pressure increases, also shown in Fig. 7. As $CO_2$ capture pressure is constant, the power consumption of $CO_2$ compressor decreases because of the flue gas flow rate decreases. Fig. 8 shows the change trend of $CO_2$ quantity captured by the system with LNG regasification pressure. The mathematical explanation can be found in Section 3. From Eq. (2), Eq. (9) and Eq. (10), the specific quantity of $CO_2$ recovery also can be written as

$$\alpha = \frac{(h_{RC21} - h_{RC24})(h_{L4} - h_{L3})}{(h_{RC23} - h_{RC22})(h_{C3} - h_{C2})} \tag{39}$$

Specific enthalpy is only the function of temperature and pressure of the working fluids, thus the negative feedback of $(h_{L4} - h_{L3})$ in Eq. (39) with increase of LNG regasification pressure leads to the decrease of $CO_2$ quantity captured by the system.

The exergy loss of the overall system decreases along with LNG regasification pressure increases. From Fig. 4, highest exergy losses associated with the heat transfer process with temperature difference in heat exchangers. Therefore, the change of exergy losses in heat exchangers along with LNG regasification pressure are calculated and shown in Fig. 9. It can be seen that CD1 is the dominant exergy loss unit among the four in heat exchangers of the system. Because of LNG regasification temperature can be determined by regasification pressure in vapor—liquid area, the augment of LNG regasification pressure should reduce the temperature difference in CD1. Consequently, as the LNG flow rate is constant, the exergy loss of CD1 falls down which leading to the reduction of exergy in the overall system along with LNG regasification pressure goes up. In VG1 and VG2, the exergy loss descend tardily with the LNG regasification pressure. In CD2, the exergy loss change trend is feebly waved with the LNG regasification pressure. Therefore, the exergy efficiency of the overall system is lifted by LNG regasification pressure. The effect of LNG regasification pressure on exergy efficiency of the system is shown in Fig. 10.

### 5.2.2. *The $CO_2$ capture pressure*

$CO_2$ capture pressure is another sensitive parameter of the system, which mainly impact the work consumption of $CO_2$ compressor and the heat release in liquefy process.

As $CO_2$ capture pressure is constant (0.15 MPa), the network output of the overall system has the maximum value of 119.42 kW when LNG regasification pressure is 1.0 MPa. Thus, for analyzing the effect of $CO_2$ capture pressure on the system performance, the LNG regasification pressure is set as 1.0 MPa.

The effect of $CO_2$ capture pressure on network output and exergy loss of the system is shown in Fig. 11. It shows that the network output of the overall system directly decreases along with the increase of $CO_2$ capture pressure; the exergy loss of the overall system has a reverse trend which is increases along with $CO_2$ capture pressure.

The $CO_2$ compressor, as the most work consumption unit in the system, is notably affected by $CO_2$ capture pressure. Fig. 12 indicates the effect of $CO_2$ capture pressure on the main work input and output units in the system, including NG turbine, RCI turbine, RCII turbine and $CO_2$ compressor. It can be seen that both the work output of NG turbine and the work input of $CO_2$ compressor increases with $CO_2$ capture pressure. However, the work outputs of RCI is nearly invariable with the change of $CO_2$ capture pressure. The work outputs of RCII reaches to the maximum when $CO_2$

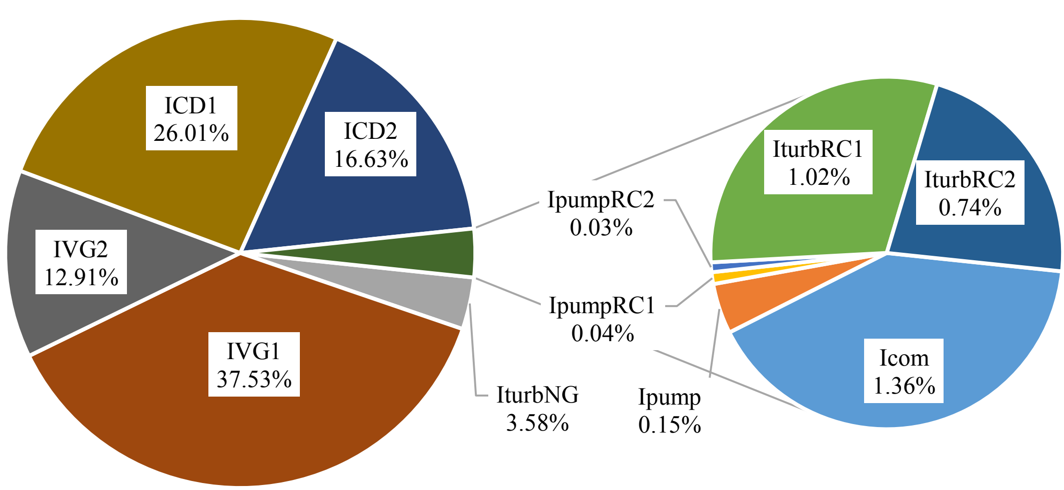


**Fig. 4.** The exergy loss percentage of components in the system (LNG regasification pressure 0.6 MPa).

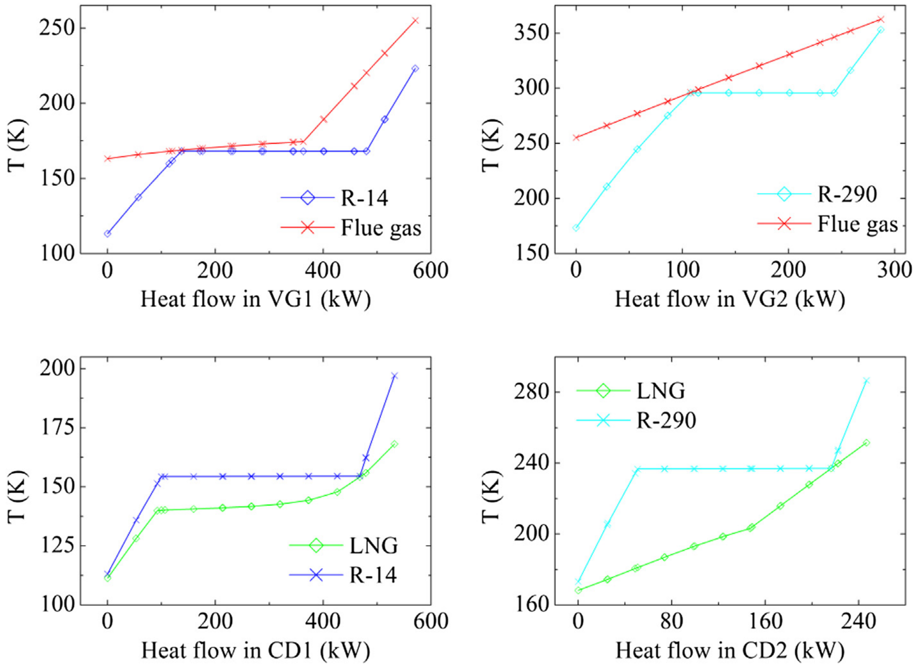


**Fig. 5.** The temperature difference and heat flow in heat exchangers (LNG regasification pressure 0.6 MPa).

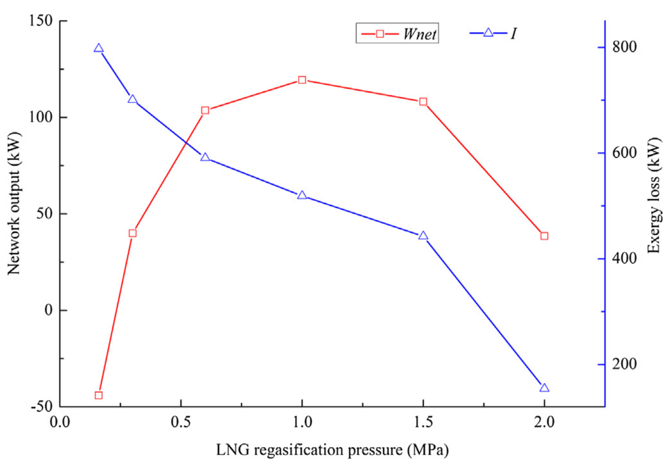


**Fig. 6.** The effect of LNG regasification pressure on network output and exergy loss of the system ($CO_2$ capture pressure 0.15 MPa).

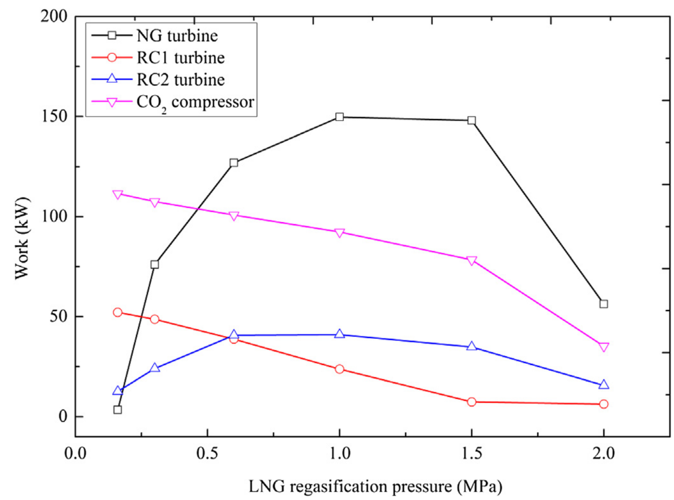


**Fig. 7.** The effect of LNG regasification on main work output/input units in the system.

capture pressure is set as 0.2 MPa. Although the work output of NG turbine increases with $CO_2$ capture pressure, the work consumption of $CO_2$ compressor climbs up more quickly. When $CO_2$ capture pressure is over 0.2 MPa, the work input of $CO_2$ compressor surpasses the work output of NG turbine. Thus, the network output of the overall system has a slump with the increase of $CO_2$ capture pressure.

The exergy loss of the overall system increases along with $CO_2$ capture pressure increases. One reason is that the exergy losses in heat exchangers of the overall system increase evidently along with $CO_2$ capture pressure which is shown in Fig. 13, especially in VG1, VG2 and CD2. The expansion of heat transfer temperature difference resulted by increase of $CO_2$ capture pressure is account for the increase of exergy losses in VG1 and VG2. In addition, for cooling down $CO_2$ adequately, the increase of $CO_2$ capture pressure leads to the increase of heat release from the flue gas to ORC II. Thus the flow rate of R-290 also grows up to fit the metabolic conditions of the flue gas. Consequently, the increased amount of LNG and R-290 exergy input results the increased exergy loss in CD2. The other reason is the increased pressure of $CO_2$ capture results the increase of exergy loss of terminational air, as analyzed in Section 5.1. Therefore, the exergy efficiency of the overall system is refrained by $CO_2$ capture pressure. The effect of $CO_2$ capture pressure on exergy efficiency is shown in Fig. 14.

Fig. 15 illustrates the effect of $CO_2$ capture pressure on $CO_2$ captured quantity of the system. The $CO_2$ captured quantity has a little augment with the increase of $CO_2$ capture pressure. The mathematical explanation also can be found though Eq. (39). The value of $h_{C2}$ is in proportion to $CO_2$ capture pressure. Furthermore, other parameters in Eq. (39) is not closely sensitive to $CO_2$ capture pressure. So the increase of $CO_2$ capture pressure could rise the value of $\alpha$ which is the $CO_2$ captured quantity in the overall system.

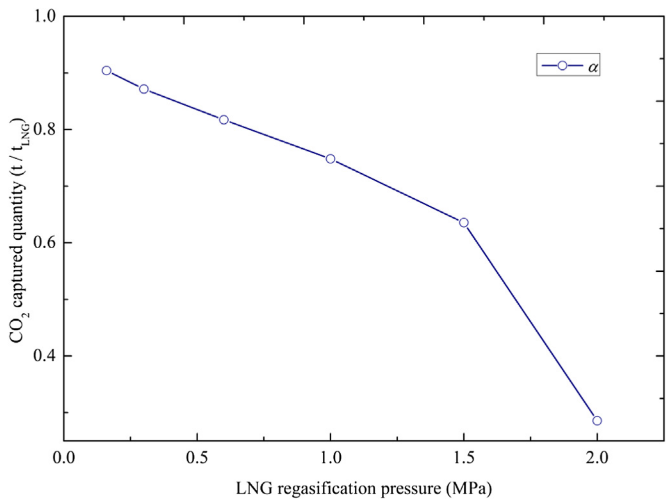


**Fig. 8.** The effect of LNG regasification pressure on $CO_2$ captured quantity of the system ($CO_2$ capture pressure 0.15 MPa).

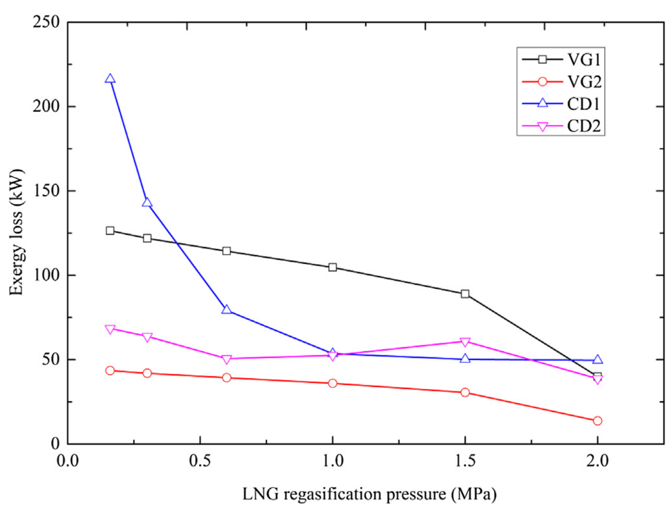


**Fig. 9.** The effect of LNG regasification pressure on exergy loss in heat exchangers of the system.

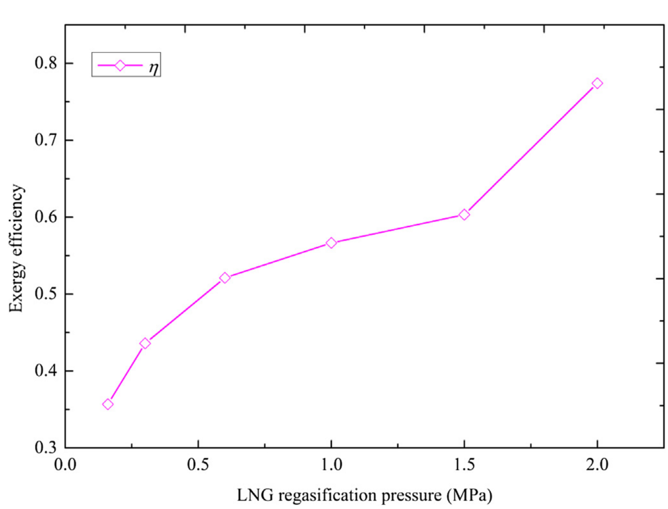


**Fig. 10.** The effect of LNG regasification pressure on exergy efficiency of the system ($CO_2$ capture pressure 0.15 MPa).

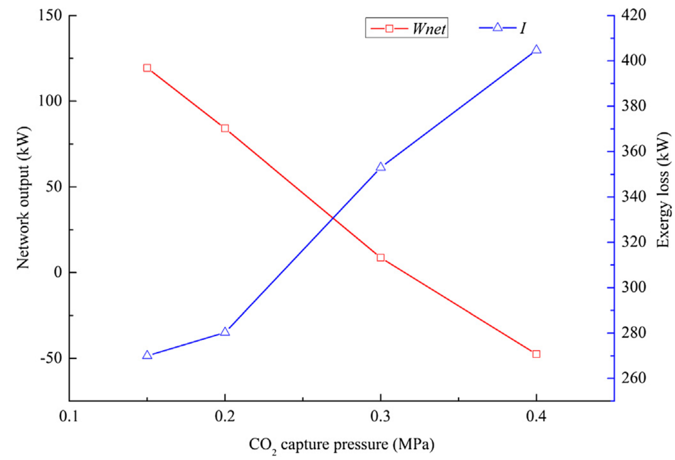


**Fig. 11.** The effect of $CO_2$ capture pressure on network output and exergy loss of the system (LNG regasification pressure 0.6 MPa).

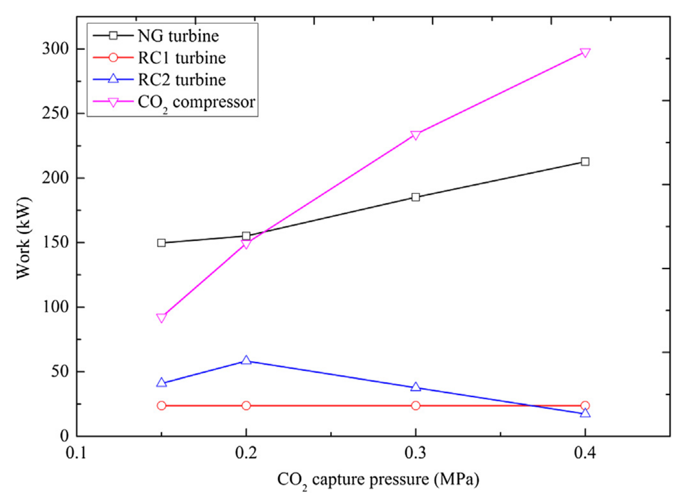


**Fig. 12.** The effect of $CO_2$ capture pressure on main work output/input components in the system.

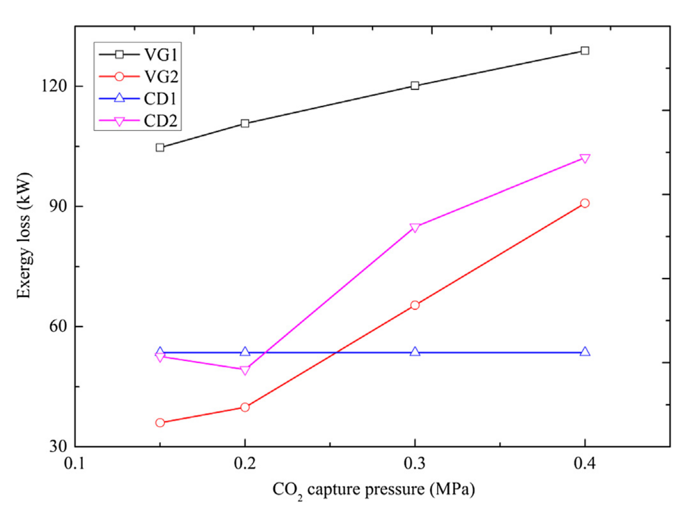


**Fig. 13.** The effect of $CO_2$ capture pressure on exergy loss in heat exchangers of the system.

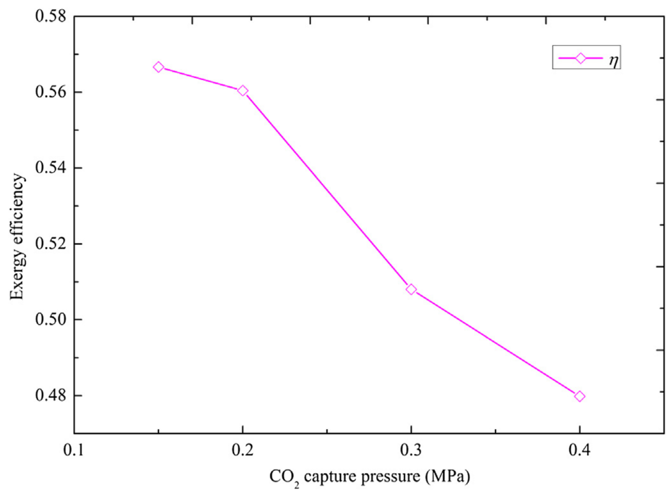


**Fig. 14.** The effect of $CO_2$ capture pressure on exergy efficiency of the system (LNG regasification pressure 0.6 MPa).

So far, the suitable of LNG regasification pressure and $CO_2$ capture pressure for the system have been found. When setting LNG regasification pressure as 1.0 MPa, $CO_2$ capture pressure as 0.15 MPa and LNG flow rate as 1 kg/s, the network output of overall system reaches to 119.42 kW with an acceptable exergy efficiency of 0.57 and $CO_2$ captured quantity of 0.75 t/$t_{LNG}$. Account for $CO_2$ discharged from magnesite processing industry in Dashiqiao Area is about 1.4 million tons per year, the system could consume 1.87 million tons of LNG for $CO_2$ capture and generate 62.03 million kilowatt-hour electric power per year.

## 6. $CO_2$ potential utilization

Carbon dioxide can be used as feedstock of many chemical products, such as methanol. Methanol ($CH_3OH$), which is considered as an important medium of chemical processing, can be synthesized via $CO_2$ hydrogenation under specific conditions [26]. Furthermore, methanol production though hydrogenation as a $CO_2$ chemical utilization method can effectively reduce direct emission of $CO_2$ [33]. In Liaoning Province, the yield of methanol is over ten thousand tons per month according to the official data. Therefore, a potential $CO_2$ utilization sub-system is also proposed, shown as Fig. 16. To avoid more $CO_2$ emission and keep low cost, hydrogen is produced by solar energy [34].

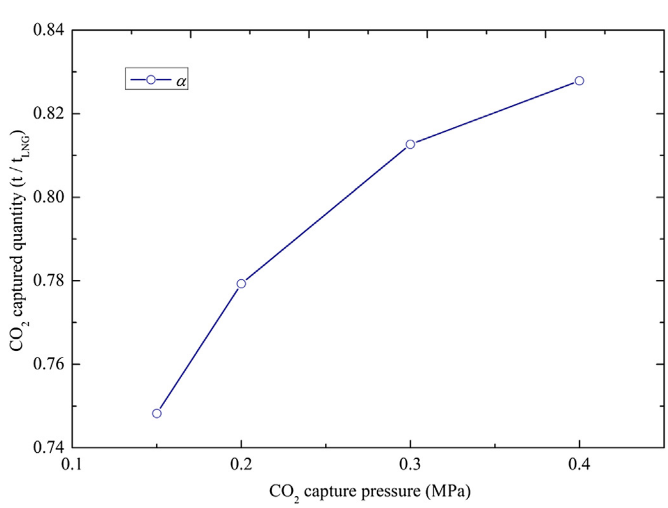


**Fig. 15.** The effect of $CO_2$ capture pressure on $CO_2$ captured quantity of the system (LNG regasification pressure 0.6 MPa).

The $CO_2$ utilization sub-system mainly consists of solar energy collector, pump (Pump RCIII), turbine (Turbine RCIII), heat exchanger (CD3), $LCO_2$ pump, alkaline water electrolyzer and reactor. The solar energy collector, the Pump RCIII, the Turbine RCIII and the heat exchanger CD3 constitutes a Rankine cycle (Rankine cycle III) which regards solar energy as heat source and liquefied carbon dioxide as heat sink. The electricity required by the water electrolyzer is generated by the Rankine cycle III. As the products of electrolysis, the hydrogen is delivered to the reactor for methanol production, and the oxygen as the by-product can be used for industrial or medical applications [35]. The liquefied $CO_2$ captured from the flue gas of magnesite processing industry, firstly, is boosted up to reaction pressure by the $LCO_2$ pump. And then, it is vaporized in CD3 by absorbing heat from the Rankine cycle III. Finally, $CO_2$ is hydrogenated and transformed into methanol and water in the reactor. The reaction equation in the water electrolyzer and the reactor is shown as Eq. (40) and Eq. (41), respectively. The water generated in the reactor can be reused in the water electrolyzer for hydrogen production.

$$2H_2O \rightarrow 2H_2 + O_2 \tag{40}$$

$$CO_2 + 3H_2 \rightarrow CH_3OH + H_2O \tag{41}$$

The design conditions of the $CO_2$ utilization sub-system is shown in Table 3. Accordingly, the power output of the Rankine cycle III under the design conditions is calculated as 102.7 kW by equations in Section 3.2. According to the MTU electrolyzer introduced by Wendt and Kreysa [36], the power required of the electrolyzer is 48.89 kWh/kg $H_2$. Thus, the power generated by the Rankine cycle III can maximize the production of hydrogen to 2.10 kg/h. That means only 0.7 kg/h $CO_2$ can be reformed to methanol in the reactor. The crux is that the power generated by the Rankine cycle III used liquefied carbon dioxide as heat sink cannot product enough hydrogen for $CO_2$ hydrogenation to methanol.

There are two possible methods to alleviate this situation, also shown in Fig. 16: ① Producing hydrogen by other technologies for supplement, such as PV/electrolysis technology; ② Appling redundant $CO_2$ for other utilizations, such as fertilizer production. PV/electrolysis is a technology that indirectly uses solar energy based on photovoltaic electrolysis for splitting hydrogen from water. It is an important research direction of hydrogen production by renewable energy [37]. And furthermore, the abundant geothermal resource in Liaoning Province is also a good renewable energy option for hydrogen production [38]. On the other hand, since Liaoning Province is a main producing area of maize in China, carbon dioxide can be used as fertilizer for promoting the growth of crops like maize [39].

In general, $CO_2$ captured from the magnesite processing industry can be used for raw material of methanol and fertilizer production. However, the efficiency of the $CO_2$ utilization sub-system, such as the solar-hydrogen efficiency and the exergy efficiency, is needed further investigation.

## 7. Conclusion

In this paper, a novel system of LNG cold energy utilization for generating power and capturing $CO_2$ is reported. Yingkou City in Liaoning Province (China) is set as the basic case for investigating to capture exhaust $CO_2$ discharged from magnesite processing industry for LNG cold energy recovery. A twin-stage organic Rankine

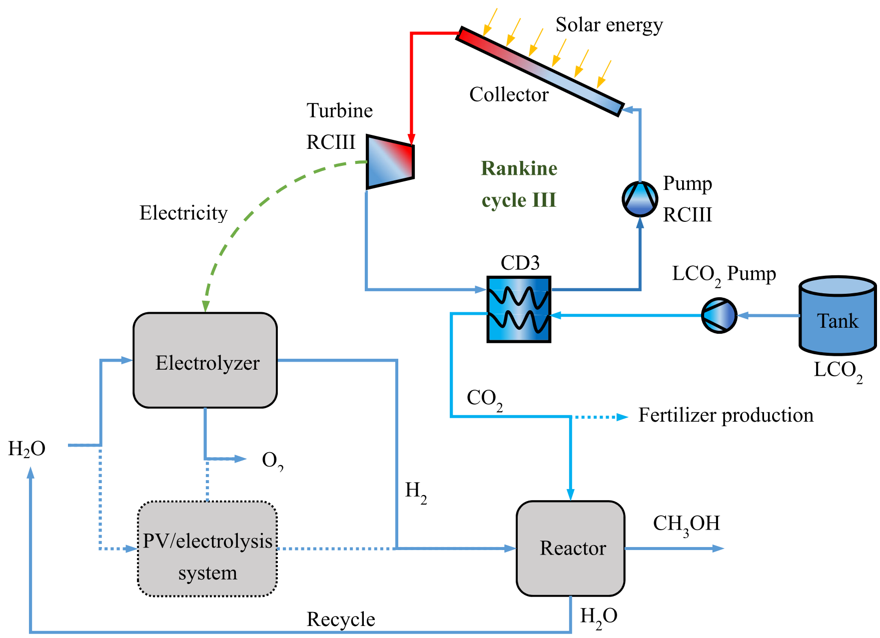


**Fig. 16.** The scheme of $CO_2$ utilization sub-system.

cycle is employed for power generation sub-system using LNG as heat sink and exhaust gas as heat source. The effects of LNG regasification pressure and $CO_2$ capture pressure on the performance of the system are examined based on the exergy analysis method. The exergy losses, exergy efficiency and network output of the system are also studied. The suitable working condition of the system is 1.0 MPa of LNG regasification pressure and 0.15 MPa of $CO_2$ capture pressure with the maximum network output of 119.42 kW. The LNG imported in Xianrendao Port can afford to capture $CO_2$ from the magnesite processing industry at Dashiqiao Area (1.4 Mt per year) by using the system under the specific conditions. In addition, the system can reach an acceptable exergy efficiency of 0.57, also can provide considerable electric power (62.03 million kWh) and liquid $CO_2$ products (1.40 Mt per year). The $CO_2$ captured from the magnesite processing industry can be used as raw material for chemical productions in Liaoning Province, such as methanol and fertilizer.

**Table 3**
The design parameters of the $CO_2$ utilization sub-system.

| Rankine cycle III | |
|---|---|
| Working fluid | R-500 |
| RC3 pump inlet temperature (K) | 173.15 |
| RC3 pump inlet pressure (MPa) | 0.31 |
| RC3 pump outlet pressure (MPa) | 18.5 |
| RC3 turbine outlet pressure (MPa) | 0.313 |
| RC3 turbine outlet temperature (K) | 283.15 |
| Heat exchanger pressure drop (MPa) | 0.003 |
| Collector outlet temperature (K) | 494.85 |
| $CO_2$ mass flow (kg/s) | 0.75 |
| $CO_2$ outlet temperature (K) | 278.15 |
| **Alkaline water electrolyzer** [36] | |
| Pressure (MPa) | 3.0 |
| Temperature (K) | 403.15 |
| **Reactor** [40] | |
| $H_2/CO_2$ (molar composition) | 3 |
| Pressure (MPa) | 3.0 |
| Temperature (K) | 513.15 |

## Acknowledgment

The authors wish to express their deep gratitude to researchers from SEP Key Laboratory of ECO-Industry of Northeastern University in China for cooperating in this study.

This work is supported by the National Science and Technology Support Project (2015BAB18B00).

## References

[1] Kumar S, Kwon H-T, Choi K-H, Lim W, Cho JH, Tak K, et al. LNG: an eco-friendly cryogenic fuel for sustainable development. Appl Energy 2011;88(12):4264–73.
[2] Romero Gómez M, Ferreiro Garcia R, Romero Gómez J, Carbia Carril J. Review of thermal cycles exploiting the exergy of liquefied natural gas in the regasification process. Renew Sustain Energy Rev 2014;38:781–95.
[3] Kanagawa T. Japan's LNG utilization and environmental efforts. Tokyo, Japan: The Japan Gas Association; 2008.
[4] Dispenza C, Dispenza G, La Rocca V, Panno G. Exergy recovery during LNG regasification: electric energy production – part one. Appl Therm Eng 2009;29(2–3):380–7.
[5] Dispenza C, Dispenza G, Rocca VL, Panno G. Exergy recovery during LNG regasification: electric energy production – part two. Appl Therm Eng 2009;29(2–3):388–99.
[6] Szargut J, Szczygiel I. Utilization of the cryogenic exergy of liquid natural gas (LNG) for the production of electricity. Energy 2009;34(7):827–37.
[7] Choi I-H, Lee S, Seo Y, Chang D. Analysis and optimization of cascade Rankine cycle for liquefied natural gas cold energy recovery. Energy 2013;61:179–95.
[8] Gómez MR, Garcia RF, Gómez JR, Carril JC. Thermodynamic analysis of a Brayton cycle and Rankine cycle arranged in series exploiting the cold exergy of LNG (liquefied natural gas). Energy 2014;66:927–37.
[9] Dong H, Zhao L, Zhang S, Wang A, Cai J. Using cryogenic exergy of liquefied natural gas for electricity production with the Stirling cycle. Energy 2013;63:10–8.
[10] Rao W-J, Zhao L-J, Liu C, Zhang M-G. A combined cycle utilizing LNG and low-temperature solar energy. Appl Therm Eng 2013;60(1–2):51–60.
[11] Liu Y, Guo K. A novel cryogenic power cycle for LNG cold energy recovery. Energy 2011;36(5):2828–33.
[12] Lee U, Kim K, Han C. Design and optimization of multi-component organic Rankine cycle using liquefied natural gas cryogenic exergy. Energy 2014;77:520–32.
[13] Sun H, Zhu H, Liu F, Ding H. Simulation and optimization of a novel Rankine power cycle for recovering cold energy from liquefied natural gas using a mixed working fluid. Energy 2014;70:317–24.
[14] Wang J, Wang J, Dai Y, Zhao P. Thermodynamic analysis and optimization of a transcritical $CO_2$ geothermal power generation system based on the cold energy utilization of LNG. Appl Therm Eng 2014;70(1):531–40.

[15] Zhang N, Lior N. A novel near-zero $CO_2$ emission thermal cycle with LNG cryogenic exergy utilization. Energy 2006;31(10–11):1666–79.
[16] Liu M, Lior N, Zhang N, Han W. Thermoeconomic analysis of a novel zero-$CO_2$-emission high-efficiency power cycle using LNG coldness. Energy Convers Manage 2009;50(11):2768–81.
[17] Zhang N, Lior N, Liu M, Han W. COOLCEP (cool clean efficient power): a novel $CO_2$-capturing oxy-fuel power system with LNG (liquefied natural gas) coldness energy utilization. Energy 2010;35(2):1200–10.
[18] Alabdulkarem A, Hwang Y, Radermacher R. Energy consumption reduction in $CO_2$ capturing and sequestration of an LNG plant through process integration and waste heat utilization. Int J Greenh Gas Control 2012;10:215–28.
[19] Bray EL. Mineral commodity summaries-magnesium compounds. In: Specialist UMC; 2014.
[20] Xiaomeng J. Study on advanced energy conversion technology for fused magnesia smelt from magnesite and the crystallization process and periclase. Shenyang, China: Northeastern University; 2011.
[21] Magnesia material network of China http://www.lnmo.com.cn.
[22] Yue Z, Hao Z, Xiaowen H. Study on $CO_2$ emission investigation and reduction measure in Liaoning Province. J Anhui Agric Sci 2010;38(23):12357–60.
[23] Qi G, Shan F, Li Q, Yu J. Energy saving by applying 3000 kVA electric arc furnace in fused magnesia production. In: Chinese Materials Conference 2012; 2012. Taiyuan, China.
[24] Li L, Zhao N, Wei W, Sun Y. A review of research progress on $CO_2$ capture, storage, and utilization in Chinese Academy of Sciences. Fuel 2013;108: 112–30.
[25] Xu G, Yang Y-p, Ding J, Li S, Liu W, Zhang K. Analysis and optimization of $CO_2$ capture in an existing coal-fired power plant in China. Energy 2013;58: 117–27.
[26] Jin H, Gao L, Han W, Hong H. Prospect options of $CO_2$ capture technology suitable for China. Energy 2010;35(11):4499–506.
[27] Dauber F, Span R. Modelling liquefied-natural-gas processes using highly accurate property models. Appl Energy 2012;97:822–7.
[28] Brown JS, Brignoli R, Daubman S. Methodology for estimating thermodynamic parameters and performance of working fluids for organic Rankine cycles. Energy 2014;73(0):818–28.
[29] Li C, Gillum C, Toupin K, Donaldson B. Biomass boiler energy conversion system analysis with the aid of exergy-based methods. Energy Convers Manage 2015;103:665–73.
[30] Lin W, Zhang N, Gu A. LNG (liquefied natural gas): a necessary part in China's future energy infrastructure. Energy 2010;35(11):4383–91.
[31] CNOOC, China National Offshore Oil Corporation. http://www.cnooc.com.cn/.
[32] Xia G, Sun Q, Cao X, Wang J, Yu Y, Wang L. Thermodynamic analysis and optimization of a solar-powered transcritical $CO_2$ (carbon dioxide) power cycle for reverse osmosis desalination based on the recovery of cryogenic energy of LNG (liquefied natural gas). Energy 2014;66:643–53.
[33] Fan J-L, Zhang X, Zhang J, Peng S. Efficiency evaluation of $CO_2$ utilization technologies in China: a super-efficiency DEA analysis based on expert survey. J $CO_2$ Util 2015. http://dx.doi.org/10.1016/j.jcou.2015.01.004.
[34] Guerra L, Gomes J, Puna J, Rodrigues J. Preliminary study of synthesis gas production from water electrolysis, using the ELECTROFUEL® concept. Energy 2015;89:1050–6.
[35] Kato T, Kubota M, Kobayashi N, Suzuoki Y. Effective utilization of by-product oxygen from electrolysis hydrogen production. Energy 2005;30(14):2580–95.
[36] Wendt HKG. Electrochemical engineering, science and technology in chemical and other industries. Berlin Heidelberg: Springer; 1999.
[37] Djafour A, Matoug M, Bouras H, Bouchekima B, Aida MS, Azoui B. Photovoltaic-assisted alkaline water electrolysis: basic principles. Int J Hydrogen Energy 2011;36(6):4117–24.
[38] Yilmaz C, Kanoglu M. Thermodynamic evaluation of geothermal energy powered hydrogen production by PEM water electrolysis. Energy 2014;69:592–602.
[39] Manderscheid R, Erbs M, Weigel H-J. Interactive effects of free-air $CO_2$ enrichment and drought stress on maize growth. Eur J Agron 2014;52:11–21.
[40] Lei H, Nie R, Wu G, Hou Z. Hydrogenation of $CO_2$ to $CH_3OH$ over Cu/ZnO catalysts with different ZnO morphology. Fuel 2015;154:161–6.


## Nomenclature

*$\alpha$:* specific quantity of $CO_2$ recovery, t/$t_{LNG}$
*$\eta$:* exergy efficiency
*E:* exergy rate, kW
*h:* specific enthalpy, kJ/kg
*$h_0$:* reference enthalpy, kJ/kg
*I:* exergy loss rate, kW
*m:* mass flow rate, kg/s
*Q:* heat flow rate, kW
*s:* specific entropy, kJ/(kg K)
*$s_0$:* reference entropy, kJ/(kg K)
*T:* temperature, K
*W:* power, kW

*Abbreviations*

*$CO_2$:* carbon dioxide
*$LCO_2$:* liquefied carbon dioxide
*LMTD:* log mean temperature difference
*LNG:* liquefied natural gas
*NG:* natural gas
*RC:* rankine cycle